

# Network and Seiberg Duality

---

Dan Xie♣ and Masahito Yamazaki♠

♣*Institute for Advanced Study, Princeton, NJ 08540, USA*

♠*Princeton Center for Theoretical Science, Princeton University, Princeton NJ 08544, USA*

*E-mail:* [dxie@ias.edu](mailto:dxie@ias.edu), [masahito@princeton.edu](mailto:masahito@princeton.edu)

**ABSTRACT:** We define and study a new class of 4d  $\mathcal{N} = 1$  superconformal quiver gauge theories associated with a planar bipartite network. While UV description is not unique due to Seiberg duality, we can classify the IR fixed points of the theory by a permutation, or equivalently a cell of the totally non-negative Grassmannian. The story is similar to a bipartite network on the torus classified by a Newton polygon. We then generalize the network to a general bordered Riemann surface and define IR SCFT from the geometric data of a Riemann surface. We also comment on IR R-charges and superconformal indices of our theories.

---

## Contents

<b>1</b>	<b>Introduction</b>	<b>1</b>
<b>2</b>	<b>Planar Bicolored Network</b>	<b>3</b>
2.1	Network and Moves	3
2.2	The Definition of the Theories	4
2.3	Reduced Network	8
2.4	Classification by Permutations	10
2.5	Totally Non-negative Grassmannian	11
2.6	Comments on Non-Planar Networks	13
<b>3</b>	<b>Bordered Riemann Surface and Network</b>	<b>15</b>
3.1	Open Pants Decomposition	16
3.1.1	Comparison with Gaiotto Theories	18
3.1.2	Generalizations	19
3.2	Ideal Triangulation	20
3.2.1	The Definition of the Theories	21
3.2.2	Seiberg Duality is a Flip	22
3.3	Bipartite Graph	23
<b>4</b>	<b>Properties of The Theories</b>	<b>23</b>
4.1	R-charge	24
4.2	Superconformal Index and Spin Chains	25
<b>5</b>	<b>Outlook</b>	<b>26</b>

---

## 1 Introduction

The view on constructing and studying superconformal field theory (SCFT) has changed dramatically over the last decades. Conventionally a SCFT is defined by specifying the matter content and the Lagrangian. This method, however, has a number of limitations. First, it is in many cases hard to compute physical observables in the strongly coupled region of the parameter space. Second, there are many qualitative properties of the theory not present in the Lagrangian, such as hidden symmetries which cannot be identified from the Lagrangian.<sup>1</sup> Third, the Lagrangian description is far from unique and it could take completely different forms in different corners of the parameter space, and the equivalence

---

<sup>1</sup>One famous example is the dual superconformal symmetry of  $\mathcal{N} = 4$  SYM theory [1], and another is the 3d mirror symmetry [2], where there is no Lagrangian description which manifests all the non-Abelian global symmetries acting on the Higgs and Coulomb branches.

of the different descriptions requires highly non-trivial duality properties. Moreover, there are many interesting strongly coupled field theory which one could not even write the Lagrangian in any corner, and even if you have the Lagrangian it is not really useful if it is complicated (e.g. huge gauge groups and many matters).

In the middle nineties, brane/geometric constructions are used extensively in the study of quantum field theories, and it has been discovered that highly non-trivial dualities of field theories have very nice geometric representation, for example as a rearrangement of the brane configuration [3].

More recently, a fresh perspective on quantum field theory has been emerging. The first example is the Gaiotto's construction on four dimensional  $\mathcal{N} = 2$  SCFTs [4]. Instead of specifying a Lagrangian, one specifies a genus  $g$  Riemann surface and punctures with specification of the local data. One immediate virtue is that all the UV deformations are encoded as geometric parameters of the Riemann surface and the local data defining the punctures. Moreover, the IR theory is solved by the moduli space of the Hitchin's equation defined on the surface [5, 6]. What is remarkable is that highly non-trivial S-duality of the field theory is trivialized; it corresponds to different pants decompositions of the same Riemann surface. Moreover, one only needs to know the S-duality behavior of the four punctured sphere. Once we understand this simple local piece, the whole S-duality behavior is understood by gluing/gauging this basic building block.

The second example is the three-dimensional  $\mathcal{N} = 2$  SCFT constructed from a hyperbolic 3-manifold [7–12]. Here, the 3d gauge theory is specified by an ideal triangulation and the choice of the polarization, and a gluing of tetrahedra is translated into a gauging of global symmetries in gauge theories. Different ideal triangulations are related by a sequence of local moves (2-3 moves), and each move corresponds to a 3d mirror symmetry. Moreover, the IR behavior is determined by (quantization of) the moduli space of the flat connections defined on the 3-manifold.

The third example is the four-dimensional  $\mathcal{N} = 1$  SCFT described by bipartite graphs on a two-dimensional torus (see [13–15]). The global data here is a toric Calabi-Yau 3-manifold determined from a convex polygon, and different bipartite graphs corresponding to the same geometry are related by a chain of Seiberg dualities [16], which are realized as square moves on the graph. The theories originates from the compactification of an NS5-brane intersecting with D5-branes ([17, 18], see also [19]).

While all these developments start with global geometric objects and the duality frames are understood as the different decompositions of the same object, physically it is easier to take a bottom-up approach; start with simple matter systems and gauge the flavor symmetries together to build complicated theories, and study the IR fixed point defined by the new theory. However, there are several questions about this approach. First, can we define a simple geometric object associated with the field theory so it is easy to study them? Second, the UV Lagrangian descriptions might be redundant, i.e. some of the gauge groups are decoupled in the IR. Can we find a minimal duality frame in which nothing is redundant? Third, it is hard to judge whether two complicated theories are related by a sequence of dualities, it would be nice to get a global data independent of the duality frame.

The goal of this paper is to provide a concrete answer to these questions, in a class of four dimensional  $\mathcal{N} = 1$  SCFTs. The geometric object is a planar bicolored network which is a generalization of the dimer model of the torus to the disc. Instead of starting from some global data, we just start with a random bicolored network which physically means we just randomly gauging the matter systems. There are several operations on the network which are perfectly mapped to the operations on the physical operations which do not change the IR fixed point. Therefore the physical questions are mapped to the combinatorial question of the network [20].

The minimal duality frames are identified with the reduced network and there are easy combinatorial ways of judging whether or not a theory is minimal, and of finding the reduced one. Similarly to the dimer story, different geometrical/combinatorial representations are related by Seiberg dualities [21], which are trivialized by the so-called local square move on the planar bipartite network. The duality equivalence class of our SCFTs, when the bicolored graphs are reduced, are classified by combinatorial data of a permutation (or equivalently a cell of the totally non-negative Grassmannian  $(\text{Gr}_{k,n}(\mathbb{R}))_{\geq 0}$  [20]), which are the invariant data independent of the duality frame).

We also extended our study to bordered Riemann surfaces (section 3). Here we take a top-down approach; we start with the global data, i.e. a Riemann surface, and identify the minimal duality frames. It is further shown that this class of theories could again be described by bipartite networks, this time defined on a higher genus Riemann surface. Therefore all the theories in this paper are defined from the network and in each case we have identified the global data characterizing the IR fixed point, as well as the minimal duality frames.

We will comment on the physical properties of our 4d  $\mathcal{N} = 1$  SCFTs (section 4), including the IR R-charge and the 4d superconformal index.

Towards the completion of this work we became aware of another work by S. Franco, which has some overlap with our work [22]. We have coordinated submission of our papers.

## 2 Planar Bicolored Network

In this section, we will define a quiver gauge theory from a reduced planar bicolored network<sup>2</sup>. The operations on 4d gauge theories keeping the IR fixed point, including the Seiberg duality, will be interpreted as combinatorial operations on the network. We will furthermore find permutations as the global data uniquely characterizing the IR fixed point.

### 2.1 Network and Moves

Let us begin with a (undirected) planar bicolored network  $\mathcal{G}$  (also abbreviated as a plabic network). Here a bicolored means that the vertices of the graph are colored either black or white. We will denote the number of boundary vertices by  $n$ , which will be fixed throughout the analysis below.

---

<sup>2</sup>In [20], a network means a graph together with weights associated to the edges or faces of the graph. The weights are essential in [20] but will not be necessary for the definition of the theory in this paper, hence our terminology here is that a network is synonymous with a graph.

We assume the network is connected and irreducible which means we can not separate the network into the disconnected parts, and there are no internal vertices with only one incident edge, we also exclude the case where a loop is attached on a vertex. This means the network separates the disk into faces. The closed faces are inside the disk while the open faces are on the boundary. See an example in Fig. 1.

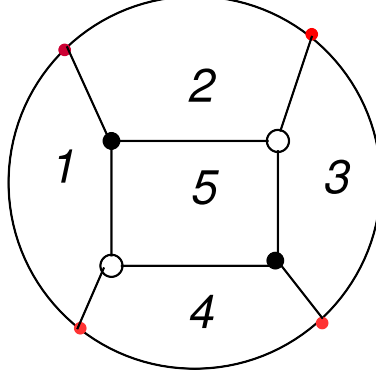


**Figure 1.** An example of a planar bicolored network on a disc with four boundary marked points.

There are several moves and reductions one can perform on networks.<sup>3</sup> The first is the square move (Fig. 2). The second is to merge or unmerge vertices of the same color (Fig. 3). The third is to remove a degree 2 vertex (Fig. 4). These three moves do not change the faces of the network. Finally, there is the so-called bubble reduction, which reduces the number of faces by one (Fig. 5).

A network is called bipartite if all the edges are connecting the vertices with different colors. It is easy to see that one can transform any network into a bipartite graph either by merging same-colored vertices or adding degree two vertices.

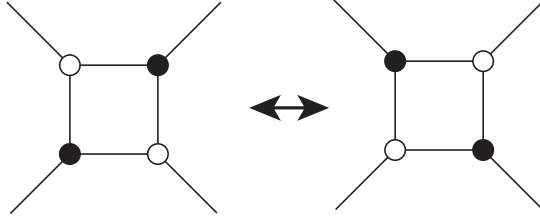


**Figure 2.** Move 1: a square move flips the color of the vertices around a square.

## 2.2 The Definition of the Theories

We will associate a 4d  $\mathcal{N} = 1$  quiver gauge theory with any connected planar bipartite network  $\mathcal{G}$ . For a non-bipartite network, one could first get a bipartite network by merging the vertices of the same colors. The rules for the bipartite network are then summarized as follows.

---

<sup>3</sup>Beside the three moves and one reduction discussed in this paper, [20] introduces two more reductions, leaf reduction and dipole reduction. These will not, however, play a rule here since we assume that the bicolored graph is connected.

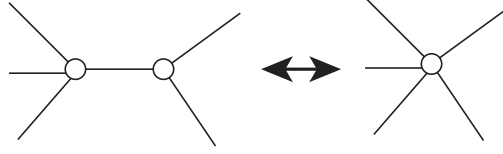


**Figure 3.** Move 2: merging/unmerging of the same-colored vertices does not change the definition of the gauge theory. Similar operation exists for black-colored vertices.



**Figure 4.** Move 3: a degree two vertices can be removed.



**Figure 5.** Reduction: bubble reduction.

1. **(gauge and flavor groups):** The network  $\mathcal{G}$  divides the plane into several regions bounded by the edges, each of which we call a face. We associate a  $SU(N)$  gauge group to each closed face, and a flavor  $SU(N)$  group for each open face, i.e. a face at the boundary.
2. **(bifundamental matters):** We associate a  $\mathcal{N} = 1$  bifundamental chiral multiplet for each edge except those edges between the white vertices and the boundary point.<sup>4</sup> The chirality is determined by the black vertices, i.e. the chiral fields form a clockwise direction around it, so the chiral fields form a counterclockwise loop around the white vertices.
3. **(superpotential terms):** We associate a superpotential term for each simple loop of the quiver diagram, so there is a superpotential term for each vertex except those white vertices connected to the boundary points.<sup>5</sup>

Notice that with the above definition, the theory does not depend on how many external edges are attached to a white vertex, hence we will restrict to the case where there is only one external edge for the white vertex without losing anything interesting. For a non-bipartite graph, instead of merging the vertices of the same colors we could also get a bipartite graph by adding degree 2 vertices. We now show that these two operations define the same IR fixed point. The two theories and the corresponding superpotential are given in Fig. 6, however, the fields  $e$  and  $f$  is massive on the left theory and we can integrate out these two fields and getting an exactly same matter content and superpotential as the right graph. This shows that the merging/unmerging operation does not change the IR theory, this also means removing a degree two vertex does not change the IR theory. With

<sup>4</sup>This will be necessary for the interpretation of a square move as a Seiberg duality.

<sup>5</sup>Here and in the following we will not be concerned with the numerical coefficient of the superpotential, as long as it is generic and non-zero. The change of those coefficients will corresponds to marginal deformations of the IR fixed points, probably along the lines of [17].

this understanding, the superpotential and the matter fields for any graph is described in Fig. 7.

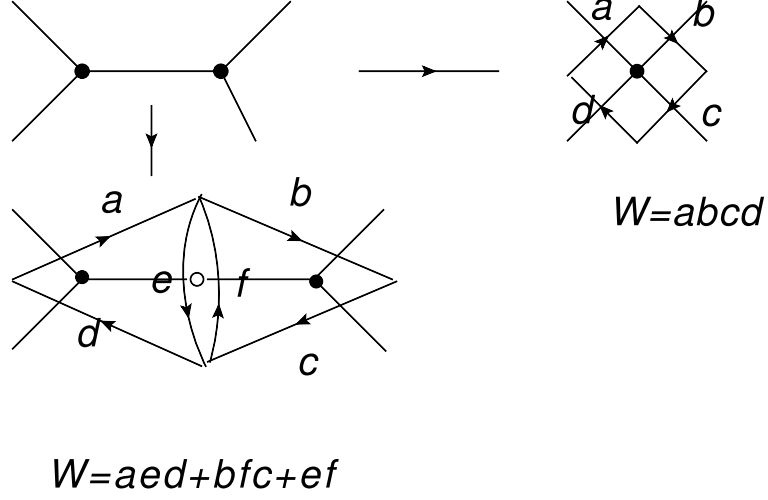


**Figure 6.** The superpotential and matter content for two different ways of making a bipartite graph.

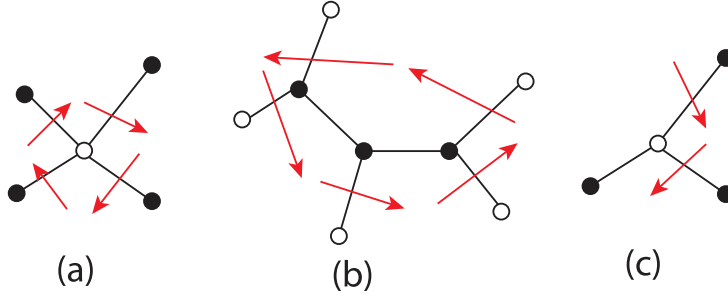


**Figure 7.** Rule for superpotential. We do not include a superpotential term when the bifundamentals around the vertex does not make a closed loop, as in the case (c).

Since the number of incoming and outgoing quiver arrows are equal for each face, and since we assign a rank  $N_c = N$  for each gauge or flavor group, our quiver gauge theory is anomaly free, and hence is a well-defined theory. We conjecture that the above defined quiver gauge theory flows to a (potentially trivial) SCFT in the IR.

#### *Seiberg Duality as a Square Move*

We have already seen that merging/unmerging of the same-colored vertices and adding degree two vertices are trivial operations which keep the IR fixed point. We would like to translate other two moves into the operations in quantum field theory and show that they would not change the IR fixed point. The square move and bubble reduction, which is the most non-trivial move, are identified with a Seiberg dualities, as will be explained below. One nice match is that for the gauge group represented by the square has  $N_f = 2N$

and  $N_f = N$  for the bubble which are the only cases where the interesting IR dynamics happen.

When  $N_f = 2N$ , after suitable merging/unmerging, we can assume that the vertices around the  $SU(N)$  gauge group has alternating colors, and are of degree 3. Let us start with the local piece of the network and assume the superpotential to have the form depicted in Fig. 8, where  $(A, B, C, D)$  represent a sequence of the fields. If there is only one field in one of the capital letters, that means that the corresponding vertex is degree 3, otherwise it has degree more than three. The superpotential has the following form

$$W = bcA + bdB + fdC + fcD + \dots \quad (2.1)$$

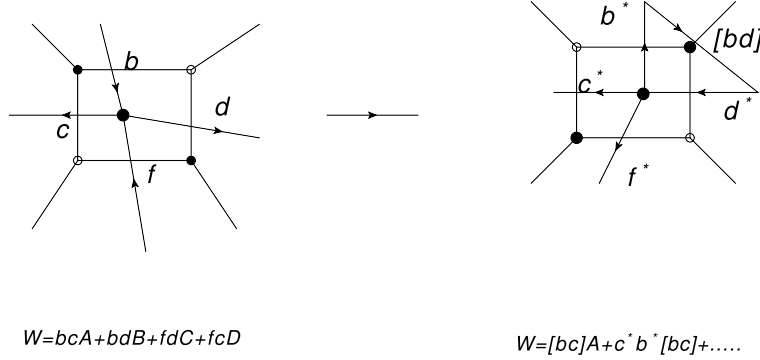


**Figure 8.** A square move of the bipartite graph is identified with a Seiberg duality.

After the Seiberg duality,  $(d, b, c, f)$  change chirality, i.e. from fundamental representation to anti-fundamental transformation [21, 23]. Pictorially, the quiver arrows for these fields are reversed, which is in agreement with the square move. There would be new mesons  $[bd]$ ,  $[fd]$ ,  $[bc]$  and  $[fc]$ , and the rank of the new gauge group is still  $N$ . The new superpotential is

$$W' = b^*c^*[bc] + b^*d^*[bd] + f^*d^*[fd] + f^*c^*[fc] + [bc]A + [bd]B + [fd]C + [fc]D + \dots \quad (2.2)$$

This is exactly equivalent to the superpotential obtained from the graph on the right of Fig. 8. To see this, one might need to integrate out the massive fields and simplify the above superpotential if one of the original sequence in  $(A, B, C, D)$  has just one field; if one of the sequences, say  $A$ , has only one field, then  $A$  and  $[bc]$  are massive, we can integrate them out, and set the  $A = b^*c^*$  in the superpotential, which is exactly the one given by the graph after merging the vertices.

When there is a bubble, then the gauge group represented by it has  $N_f = N_c$ , so there is a mass gap in the IR and the gauge group is decoupled. The IR physics is nicely interpreted formally as the Seiberg duality where the dual gauge group has rank zero and can be decoupled, and the only low-energy degrees of freedom is the meson field. It can be checked the dual theory after decoupling of the gauge group is exactly the same as the one described by the graph after bubble reduction, and the meson field is represented by an edge of the quiver diagram connecting the two faces.



All the geometric data of the network are mapped perfectly to the gauge theory description, and the moves and reductions are mapped to the gauge theory operations which do not change the IR fixed point. we summarize the mapping in Table 1.

network	gauge theory
closed face	gauge group
open face	flavor group
edge	bifundamental matter
vertex	superpotential term
merging/unmerging	IR theory unchanged
adding/removing degree two vertex	IR theory unchanged
square move	Seiberg duality on $N_f = 2N$
bubble reduction	Seiberg duality on $N_f = N$

**Table 1.** Dictionary between networks and gauge theories.

### 2.3 Reduced Network

We have defined a  $\mathcal{N} = 1$  theory for any connected plabic graph. However, the Lagrangian description of the gauge theory could be very redundant, i.e. one of the gauge groups could decouple in other duality frames. It would be nice to have some ways to find the minimal duality frame, where we could not further reduce the number of gauge groups and matter fields. Since the gauge theory operations which do not change the IR fixed point have been mapped to geometric operations on the network, the above-mentioned task is translated to a combinatorial study of the network, which has been studied in full detail in the mathematical literature.

We call a network reduced<sup>6</sup> when one cannot reduce the number of faces by the four moves/reduction above; the gauge theory description corresponding to this type of network is exactly the minimally duality frame we want to find. It seems hard to judge whether a network is reduced or not from this definition, i.e. to judge whether a complicated quiver gauge theory to be reduced or not. Fortunately there is an easy combinatorial algorithm to achieve this task on the network, and therefore we have a nice way of finding the minimal duality frame of a quiver gauge theory. Before describing the method, one needs to introduce two objects on our network. First, a zig-zag path<sup>7</sup> is a path on the network which turns maximally left at white vertex and turns maximally right at black vertex (Fig. 9). These paths come in from boundary points, and again go out to boundary points after several turns.

The second is a strand.<sup>8</sup> Place one vertex on each internal edge and connect the dots around each vertex. Take the clockwise orientation for segments around the white vertex and counterclockwise orientation for the black vertex, see Fig. 10 for illustration. The

<sup>6</sup>This is also called minimal in the literature.

<sup>7</sup>This is called a trip in [20], and is also called a train track in the literature.

<sup>8</sup>In some literature a strand is meant to be a zig-zag path in the definition here.

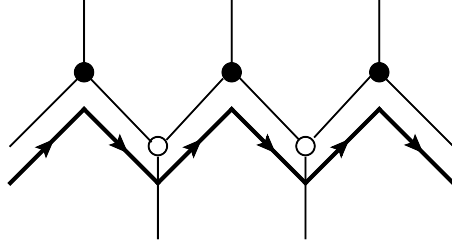


**Figure 9.** A zig-zag path which is turning left at white vertex and turning right at the black vertex.

network is replaced by another graph with all vertices degree four. A strand is defined as an oriented path such that it represents the zig-zag path (see Fig. 10).

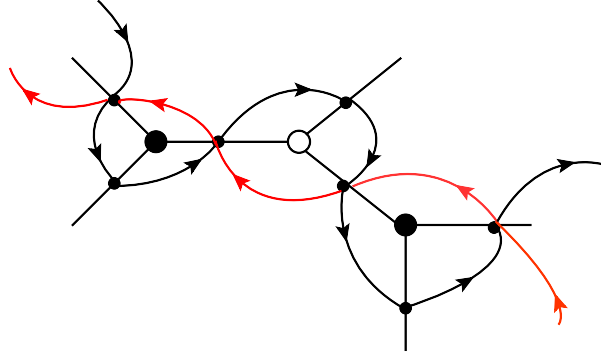


**Figure 10.** A strand for a bipartite network. Put one vertex on each edge and connect these dots around each vertex. The orientation is taken to clockwise for the white vertex and counterclockwise direction for the black vertex.

Now we can introduce the criteria for a network to be reduced [20, section 13]: there is no bad configuration of strands as described in Fig. 11; moreover, there is no closed zig-zag loop in our network. If there are bad strand configurations, then one can find a bubble after a sequence of the moves, notice that the strand structure is only changed by bubble reduction. There is a canonical way of finding and eliminating bubbles. We draw the strand on the glued network and do square moves on each bounded area of the bad strand configuration shown in the Fig. 11, bubbles will appear at some stage and we eliminate it using bubble reduction. The network become minimal after eliminating all the bubbles in this way. A useful property of a reduced planar bicolored network, when the network is



**Figure 11.** The bad configurations for the strand, forbidden in reduced bicolored graphs.

connected, is that we have

$$V - E + F = 1 , \quad (2.3)$$

where  $V, E, F$  are the number of internal vertices, edges and faces of  $\mathcal{G}$ , respectively. In the example of Fig. 1 we have  $V = 4, E = 8, F = 5$ .

The reduction is rather powerful, and a complicated network may be substantially simplified, see an example in Fig. 12. This result is rather remarkable from the gauge theory point of view, since the initial gauge theory with a huge number of gauge groups reduces to a single gauge group in the minimal duality frame!

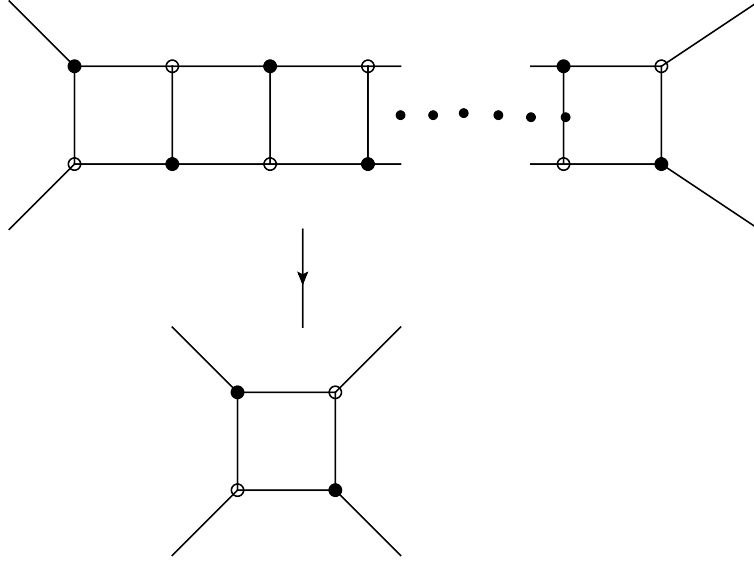


**Figure 12.** By combining the moves and the bubble reduction, we could sometimes simplify a bicolor graph considerably.

## 2.4 Classification by Permutations

We have described how to find a minimal duality frame for any quiver gauge theory defined by the network: it corresponds to the reduced network. However, the minimal duality frame is not unique, it might be possible that there are many minimal duality frames. It would be really nice if there is a way to judge whether two minimal quiver gauge theories describe the same IR fixed point.

What we want is a global characterization of the IR fixed points, as emphasized in introduction; we need an algorithm to determine, given two reduced planar bicolor networks  $\mathcal{G}$  and  $\mathcal{G}'$ , whether the two could be related by a sequence square moves. In other words we would like to extract some global data from a reduced planar bicolor graph such that two graphs are related by the moves if and only if these data match. Fortunately, there is already an answer in mathematics literature [20], which we will now explain.

Let us first label the boundary points from 1 to  $n$  (this is defined modulo translation ambiguities). Then each zig-zag path (strand) starting from point  $i$  will reach another

point  $j$ . Note that this is a one-to-one map. For example, if two paths from  $i$  and  $j$  end up the same point  $k$ , we can go backwards in the path  $k$  and find that  $i = j$ . This means that our network  $\mathcal{G}$  defines a permutation, which we denote by  $\pi_{\mathcal{G}}$ .<sup>9</sup>

Now we have the following theorem ([20, Theorem 13.4]), which provides a very simple criterion to judge whether two quiver gauge theory associated with two reduced network flow to the same IR fixed point: suppose we have two reduced planar bicolored networks  $\mathcal{G}, \mathcal{G}'$  with the same number of boundary vertices. Then  $\mathcal{G}'$  is obtained by a sequence of square moves from  $\mathcal{G}$  if and only if these two networks have the same permutation (up to a cyclic shift):  $\pi_{\mathcal{G}} = \pi_{\mathcal{G}'}$  (see Fig. 13 for an example).<sup>10</sup> This classification is quite powerful, since there are only a finite possible number of permutation of  $n$  if we fix  $n$ .<sup>11</sup>

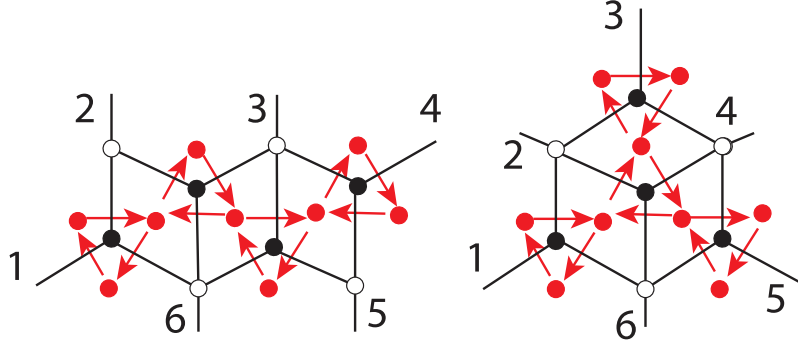


**Figure 13.** The two bipartite graphs are related by a sequence of moves, and define the same IR fixed point. Correspondingly, the two graphs give the same permutation  $\pi : \{1, 2, 3, 4, 5, 6\} \rightarrow \{3, 4, 5, 6, 1, 2\}$ .

There is an inverse to this construction; not only can one identify the permutation from a given network, but we can also construct a network from a given permutation (see [24] and [20, section 6]). We first write  $1, 1', 2, 2', \dots, n, n'$  along the boundary of the disc. We then draw paths from  $i$  to  $\pi(i)'$  such that the paths always intersect at a triple intersection point. We can then place white vertices at the triple intersection points, and black vertices to each region surrounded by the paths in a clockwise orientation (Fig. 14).

## 2.5 Totally Non-negative Grassmannian

We have seen that our theory is defined from a (decorated) permutation. Interestingly, it is known that such an object is in one-to-one correspondence with a cell of the totally non-negative Grassmannian.

<sup>9</sup>Actually in [20] this theorem is stated for a decorated permutation, not an ordinary permutation. Here a decorated permutation is a pair  $\pi \in \mathfrak{S}_n$  together with a coloring function  $\text{col}$  from the fixed point set  $\{i | \pi(i) = i\}$  to  $\{1, -1\}$ . The coloring is chosen such that if the strand for the zigzag path is a counterclockwise loop (reps., clockwise) loop, then the fixed point  $i$  is colored in black  $\text{col}(i) = 1$  (reps., white and  $\text{col}(i) = -1$ ). Such a fixed point is associated with a lollipop in the bicolored network, but we have assumed already that this does not happen (recall section 2.1), and hence we can disregard the decoration in this paper.

<sup>10</sup>It is important that  $\mathcal{G}, \mathcal{G}'$  are reduced here, since bubble reduction 5 changes the permutation.

<sup>11</sup>There are many more possibilities if we lift the condition that the planar network is connected (see also footnote 9).

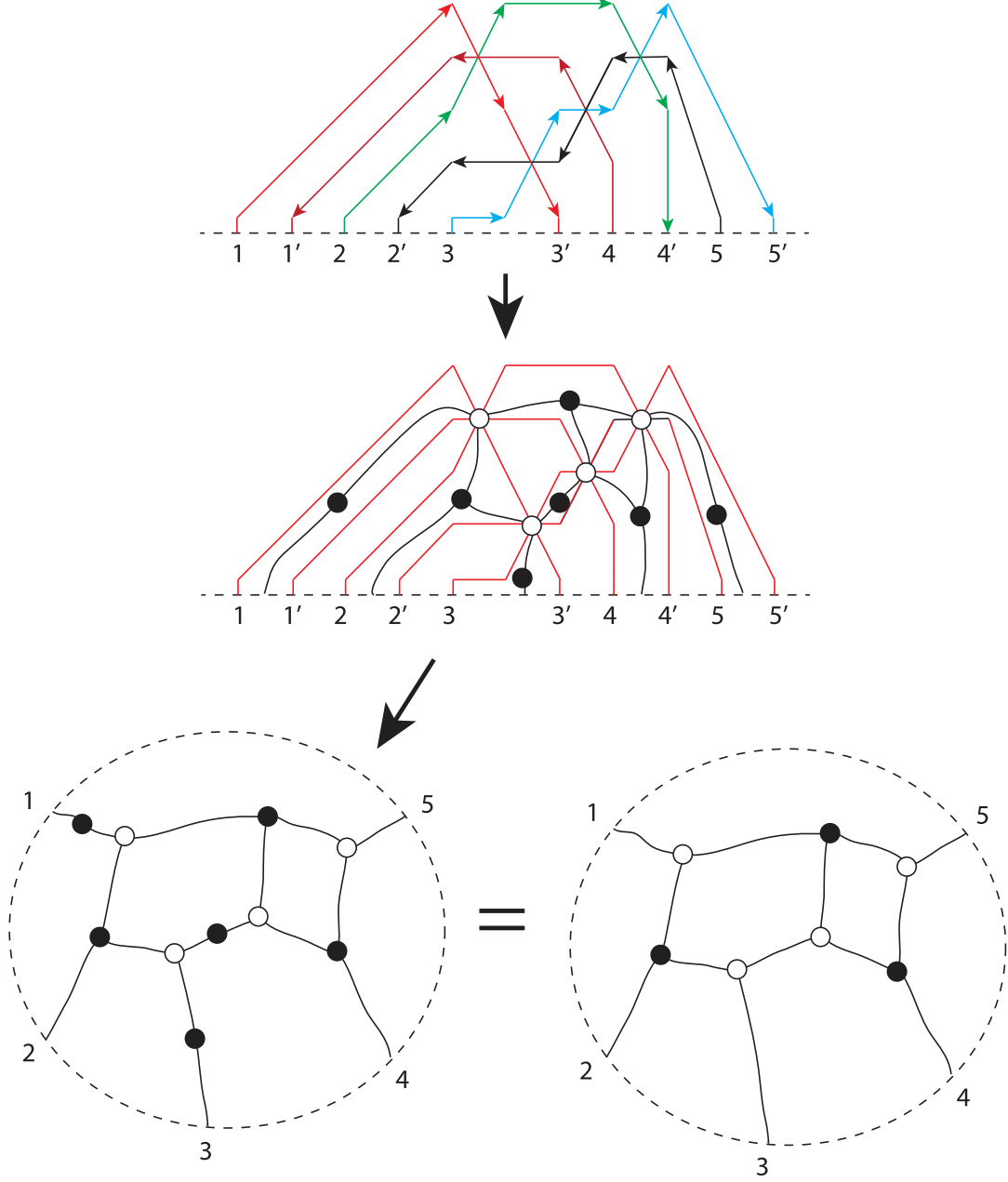


**Figure 14.** The inverse map, constructing a planar bicolored network from a permutation.

Recall that a Grassmannian manifold  $\text{Gr}_{k,n} := \text{Gr}_{k,n}(\mathbb{R})$  is the space of  $k$ -dimensional vector spaces inside  $\mathbb{R}^n$ . We define the non-negative Grassmannian  $(\text{Gr}_{k,n})_{\geq 0}$  as the subspace where the Plücker coordinates are all non-negative. This space  $(\text{Gr}_{k,n})_{\geq 0}$  has a cell decomposition, given by non-negative parts of the matroid strata.

The decorated permutation discussed in this paper is in one-to-one correspondence with a cell of this non-negative Grassmannian  $(\text{Gr}_{k,n})_{\geq 0}$ . Here that  $n$  is the number of

boundary punctures as defined previously, and an integer  $k$  is defined by

$$k - (n - k) = \sum \text{col}(v)(\deg(v) - 2) , \quad (2.4)$$

where  $\text{col}(v) = 1$  for black vertices and  $\text{col}(v) = -1$  for white vertices. We can verify that this integer  $k$  does not change under the moves, and hence is a well-defined data assigned to the IR fixed point. The planar examples in the previous section is the case  $k = 2$ . The Grassmannian duality  $k \rightarrow N - k$  is translated into the flip of the color of the vertices.

The moves introduced earlier does not change the cell it describes, similarly, the moves do not change the IR fixed point of the four dimensional gauge theory. So there is a correspondence between the positive cells of the Grassmannian to a four dimensional  $\mathcal{N} = 1$  gauge theory. This has some remarkable applications, for example, whenever we have a network with  $k = 1$ , the reduced gauge theory is trivial! This is because the only reduced connected network describing a cell of  $(\text{Gr}_{1,n})_{\geq 0}$  has only one white vertex with all the boundary points connected to it.

Interestingly, exactly the same mathematical structure of the totally non-negative Grassmannian, appears in the recent work on scattering amplitudes [25]. There are many formal similarities; for example, the black/white color in our story represents the chirality there. It remains to be seen, however, if there is a deeper reason why the same mathematical structure appears in two different physical setups.

## 2.6 Comments on Non-Planar Networks

The definition in this section has so far been limited to the planar networks. This raises an obvious question: can we generalize our definition to bicolored networks on more general bordered Riemann surfaces? Part of this will be discussed in section 3, but the question here is about a generalization to bicolored graphs not necessarily coming from a triangulation.

It is actually straightforward to adopt the planar definition to the more general case. Let us start with a bipartite network on a bordered Riemann surface. Some of the edges could run off to infinity at the boundary, however we impose the condition that they pass through the marked points at the boundary (see Fig. 15). We also impose the conditions that the bipartite graph is connected, and that there are no degree 1 internal edges. The graph then divides the Riemann surface into contractible faces.

We find again that a network divides the surface into faces, each of which is topologically a disc, i.e. all the faces are contractible. We can then use exactly the same rules in section 2.2 to define our 4d  $\mathcal{N} = 1$  theories. Note that the rules are local on the network, and hence does not require the global information of the surface.

While this definition is straightforward, what is missing here is the global data uniquely characterizing the IR fixed point, the counterpart of a decorated permutation. We will also need to generalize the definition of reduced graphs to non-planar networks, and prove a non-planar generalization of [20, Theorem 13.4].

We do not give an answer to this problem in general, and would like to leave it for future work. Instead we here point out that the answer to this question is known, when the Riemann surface is a torus without any boundaries. The theories in this case have

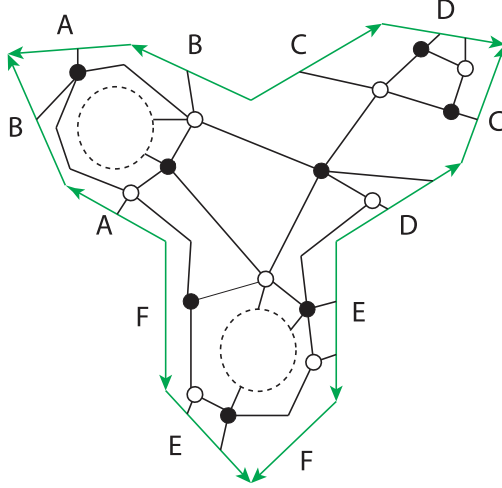


**Figure 15.** An example of network on a genus 3 surface with 2 boundaries components.

extensively been studied in the context of 4d  $\mathcal{N} = 1$  quiver gauge theories dual to toric Calabi-Yau manifolds, and the bipartite graph in this context is called a brane tiling (see [13–15] and the reviews [18, 26]).<sup>12</sup>

The definition of a zig-zag path is parallel to the planar case. Since the surface does not have any boundary components, instead of starting with a marked point on the boundary we start with an arbitrary vertex on the graph and define the zig-zag paths by following the same rule as in the planar case (turns maximally right/left at black/white vertex). Since the graph is finite, the path always will be a closed loop. By counting the winding numbers in some basis of  $H_1(\Sigma)$  (say, the  $\alpha$ -cycle and the  $\beta$ -cycle), we have a set of integers  $(n_{1,i}, n_{2,i})$  for each zig-zag path  $p_i$ . The convex polytope for these lattice points in  $\mathbb{Z}^2$  is identified with the toric diagram, which in turn defines the geometry of the toric Calabi-Yau manifold dual to these theories [13, 14]. Here the choice of the basis of  $H_1(\Sigma)$  is translated into the  $SL(2, \mathbb{Z})$  ambiguity of the torus. This convex polytope could be thought of as a torus counterpart of a decorated permutation. There is also an inverse map, to obtain a bipartite graph from a toric diagram. This has been worked out in [27], and (in the mathematical reformulation of [28]) uses essentially the same ingredient as the procedure in Fig. 14.

Moreover, under a suitable definition of a reduced graph we can show that two reduced planar bipartite graphs are connected by a sequence of the three moves in section 2.1 if and only if they correspond to the same convex polygon (up to  $SL(2, \mathbb{Z})$ -transformation and translation in  $\mathbb{Z}^2$ ), see [28, Theorem 2.5].

We can therefore regard the theories specified by bipartite graphs on  $T^2$  as a particular example of more general theories associated with a bicolored network on a bordered Riemann surface.<sup>13</sup>

<sup>12</sup>The name “brane tiling” is justified by the fact that the bipartite graph is a certain reduction of an actual brane configuration, see [18] for detailed analysis.

<sup>13</sup>See [29] for a recent discussion on 4d  $\mathcal{N} = 1$  gauge theories associated with a bipartite graph on a higher genus Riemann surface.

For a general bordered Riemann surface, we conjecture that the global data are a combination of (decorated) permutations associated with the boundary marked points, as well as the set of integers counting the winding around the non-trivial cycles of the Riemann surface. It remains to be an exciting problem to find out if this is really the case, and if these data fit nicely into a geometrical object generalizing the totally non-negative Grassmannian of [20].

In next section, we are going to study a subclass of network defined on higher genus surface with boundaries. Instead of starting with a random network, we are going to begin with some global data from the definition of the Riemann surface. This class of theories have the exactly same properties as those arising from the planar network.

### 3 Bordered Riemann Surface and Network

The goal of this section is to extend the definition of a network to higher genus bordered Riemann surface with marked point. We are going to define a 4d  $\mathcal{N} = 1$  theory  $\mathcal{T}_\Sigma^l$  for each bordered Riemann surface, for each fixed integer  $l$ . Although not quite general as the planar network, this class of network is reduced and built from the basic components, therefore they give a nice way of constructing reduced network even in the planar case.

Let us begin with a Riemann surface with boundaries, and specify a finite set of points  $M_{\text{boundary}}$ , called boundary marked points, on the boundary circles of  $\Sigma$ . Each connected component of  $\partial\Sigma$  has at least one boundary marked point; we will explain later why we exclude the boundary without marked point. The defining data of our theory is a pair  $(\Sigma, M_{\text{boundary}})$ , see Fig. 16 for an example. For notational convenience we sometimes denote this pair simply by  $\Sigma$ . In other words,  $\Sigma$  is defined by following data:

- a. the genus  $g$  of the Riemann surface;
- b. the number  $b$  of boundary components;
- c. the number of marked points  $h_i$  on each boundary.

We require there are at least three marked points for the disc, and at least one boundary component for higher genus Riemann surfaces.

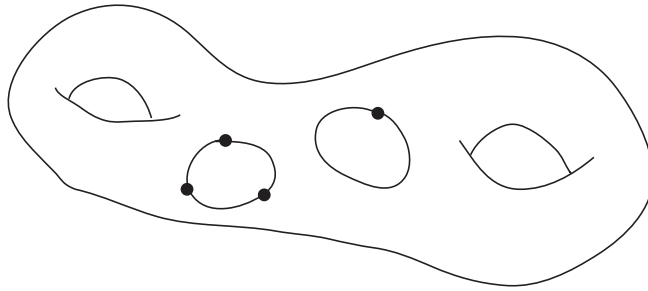


**Figure 16.** Our  $\Sigma$  is a bordered Riemann surface, whose boundary consists of disjoint union of circles. On each circle we specify at least one marked point.

Instead of directly constructing a network, we are going to define two nice equivalent combinatoric objects on a bordered Riemann surface: open pants decomposition and ideal triangulation. We are going to define  $\mathcal{N} = 1$  theories from them. The combinatoric



objects are not unique but are related by a sequence of local moves:  $s$ - $t$  duality of pants decomposition and a flip of the triangulation, both of which are equivalent to the square move introduced in previous section. This ensures that different Lagrangian descriptions are related by a sequence of Seiberg dualities, and therefore define the same IR fixed point. In the end, an equivalent bipartite network is constructed from the ideal triangulation which justifies that they are just a subclass of the theories from the network.

### 3.1 Open Pants Decomposition

This definition is in analogy of the Gaiotto's interpretation of S-duality of  $\mathcal{N} = 2$  theory [4]. The SCFT is defined by a bordered Riemann surface with marked points and there is a global  $SU(N)$  flavor symmetry associated with each marked point. We are interested in the UV Lagrangian description of the IR fixed point. In this section we focus on the case  $g = 0$ , and begin with a disc with several marked points. The Lagrangian description is derived by looking at the degeneration limit of the Riemann surface into three punctured discs. New marked points appear in the complete degeneration limit. Physically, each three punctured disc represents a matter system with  $SU(N)^3$  flavor symmetry and the gluing of the Riemann surface is interpreted as gauging the diagonal flavor symmetry associated with the marked points. Our proposal is that the  $\mathcal{N} = 1$  Seiberg duality corresponds to different degenerations of the disc.

The first step for the definition of the Lagrangian is to associate a theory  $\mathcal{T}_\Delta^l$  to each three punctured disc  $\Delta$ . We first concentrate on the case  $l = 1$ . We propose that this theory is a 4d  $\mathcal{N} = 1$  theory with global symmetry  $SU(N)^3$ , together with three  $\mathcal{N} = 1$  bifundamental chiral multiplets  $X, Y, Z$  transforming in the representation  $(N, \overline{N}, 1)$ ,  $(1, N, \overline{N})$ ,  $(\overline{N}, 1, N)$  under the  $SU(N)^3$  global symmetry. We also include a superpotential term  $W = \text{Tr}(XYZ)$ .

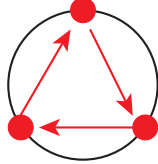


**Figure 17.** A quiver diagram for the triangle theory  $\mathcal{T}_\Delta^{l=1}$ .

It is useful to represent this by a quiver diagram in Fig. 17. Note that the theory is kept invariant under the cyclic rotation of the triangle; we simply need to change the label of bifundamental chirals. However, since the theory is chiral (except for the special case  $N = 2$ ) we do not have the symmetry under the orientation reversal of the triangle.

The second step is to glue two three punctured discs (or equivalently triangles). Let us glue two triangles  $\Delta_1, \Delta_2$  along the edge  $e$ , and define the corresponding theory  $\mathcal{T}_{\Delta_1 \cup_e \Delta_2}$  (see Fig. 18). The edge  $e$  corresponds to global symmetries  $SU(N)_1, SU(N)_2$  for the theories  $\mathcal{T}_{\Delta_1}, \mathcal{T}_{\Delta_2}$ , and by gauging the diagonal  $SU(N)$  in  $SU(N)_1 \times SU(N)_2$  we obtain a  $SU(N)$  gauge theory with six bifundamental chiral multiplets  $X_i, Y_i, Z_i$  ( $i = 1, 2$ ). This theory has a superpotential  $W = \text{Tr}(X_1 Y_1 Z_1 + X_2 Y_2 Z_2)$ , and has  $SU(N)^4$  global symmetries. At the

level of the quiver diagram, this gluing is simply to identify the two vertices of the quiver diagram corresponding to the marked point  $e$ .

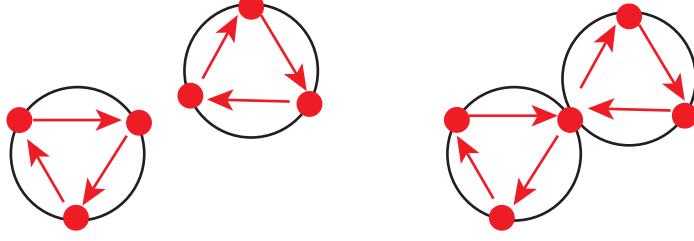


**Figure 18.** The theory for the two triangles glued along an edge.

The gluing of more three-punctured discs is similar, and there is one Lagrangian description for each degeneration. By construction the number of fundamentals and the anti-fundamentals are the same for all  $SU(N)$  gauge groups, and hence the chiral anomaly automatically vanishes for our theory  $\mathcal{T}_\Sigma$ .

We now conjecture (at least for a generic cases) these theories flow to a non-trivial IR fixed point, and we will primarily be interested in this strongly coupled theory in IR.

The basic Seiberg duality corresponds to the fourth punctured disc as shown in Fig. 19. Since there are only two degeneration limits ( $s, t$ -channels) to preserve the cyclic order, there are only two duality frames. The above interpretation is different from the  $\mathcal{N} = 2$  duality proposed in [4], where there is no cyclic order for the four punctures and we have three duality frames ( $s, t, u$ -channels).

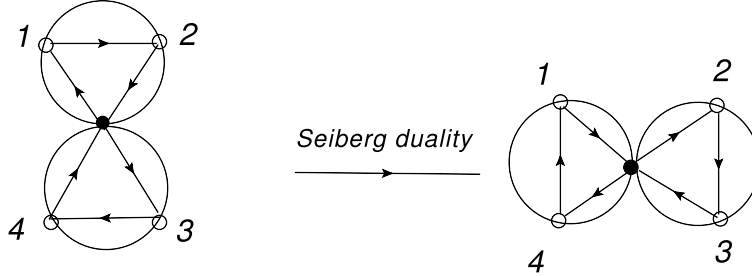


**Figure 19.** Two different degeneration limits correspond to two duality frame of the same theory.

We can also add another boundary with marked points to the Riemann surface, and there are two steps in studying the degenerations (see Fig. 20). First, there are two new marked points with the same label appearing in degenerating the hole and the Riemann surface becomes a disc, and one can find the theories in any duality frame according to the rule described earlier. We then gauge the diagonal flavor symmetries associated with the newly-appearing punctures. Following similar procedure, one can find the theory for the disc with arbitrary number of holes.

One could also consider theories from higher genus Riemann surface using the degeneration and gluing idea, however, this approach is not that illuminating and we are going to propose another easy method in next subsection.

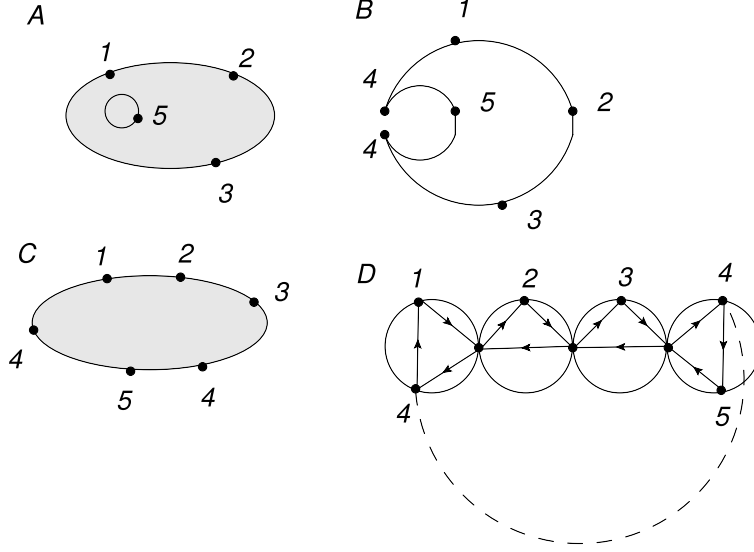


**Figure 20.** A: a Riemann surface with two boundaries and marked points, one boundary is interpreted as a hole in the disc. B: The degeneration of the hole. C: the disc with a cyclic order of marked points after the degeneration. D: One duality frame of the theory from A.

### 3.1.1 Comparison with Gaiotto Theories

As already mentioned, our definition of  $\mathcal{T}_\Sigma$  follows the same philosophy as in the 4d  $\mathcal{N} = 2$  theories defined by compactification of M5-branes on Riemann surfaces [4]. There we associate a theory  $\mathcal{T}_N$  to a trinion (three-punctured sphere), and given a pants decomposition (degeneration) of the Riemann surface the theory is defined by gluing  $\mathcal{T}_N$  theories by gauging diagonal global symmetries. Different pants decompositions correspond to different duality frames of the gauge theory. Our theory follows exactly the same step, where we used open pants instead of closed pants (see Fig. 21).

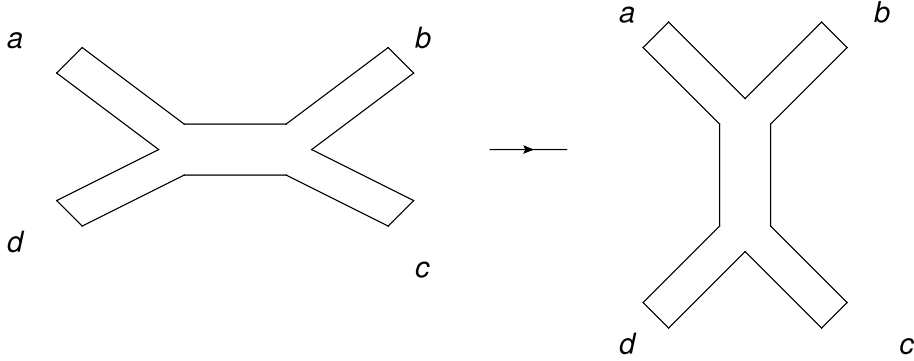


**Figure 21.** Open pants decomposition a disc with four marked points has two duality frames.

Despite the similarities it is important to keep in mind several crucial differences between (1) our theories and (2) Gaiotto theories. First, the two theories do not agree even if we take the same Riemann surface; Gaiotto theories have 4d  $\mathcal{N} = 2$ , whereas our theories have 4d  $\mathcal{N} = 1$ , and our theory for the 3-punctured sphere  $\mathcal{T}_\Delta$  is different from the  $\mathcal{T}_N$

theory. Related to this is that gluing involves gauging of a 4d  $\mathcal{N} = 1$  vectormultiplet in (1) and  $\mathcal{N} = 2$  vectormultiplet in (2). The two also uses different data in the definition; in (1) we have an integer  $l$  (as explained in next subsection) and another integer  $N$  (specifying the rank of the gauge group), whereas in (2) we have a single integer  $N$  specifying the number of M5-branes. Finally, Gaiotto theories are defined from compactification of M5-branes, whereas in our case there is apparently no such direct brane interpretation; our theory is defined purely from the combinatorial data of the triangulation.

To some readers the fact that our theories does not have (at least as of this writing) direct brane interpretation might seem like a disadvantage of our approach. However, as already emphasized in Introduction, the idea of understanding the global structure of duality symmetries in supersymmetric gauge theories from geometric data is more general than the compactification of M5-brane theories, and our theories could be thought of as one of the first examples of this sort.

### 3.1.2 Generalizations

A natural generalization is to replace the three punctured theory  $\mathcal{T}_\Delta$  such that the two theories associated with the different degenerations are related by Seiberg duality. Motivated by the seminal paper on higher Teichmüller theory by Fock and Goncharov [30],<sup>14</sup> we introduce the  $\mathcal{T}_\Delta^l$  theory show in Fig. 22. We introduce superpotential terms for any cubic loop of the quiver diagram. For example, the triangle theory  $\mathcal{T}_\Delta$  itself has  $l(l-1)/2$  superpotential terms.

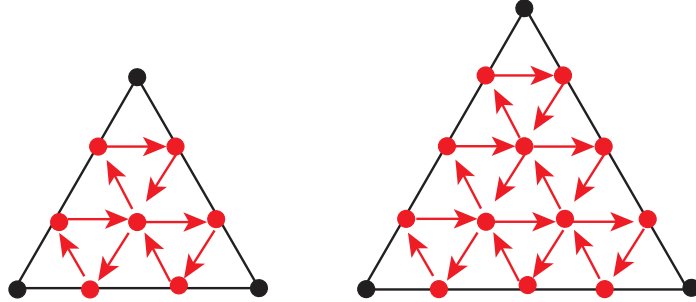


**Figure 22.** The theory  $\mathcal{T}_\Delta^l$  for  $l = 2, 3$ . There is a superpotential term for each cyclic triangle.

There are  $l$   $SU(N)$  flavor symmetries per each marked point, and the gluing of the marked points is achieved by gauging these  $l$  symmetries. We also need to include further superpotential terms for the newly formed simple loop resulting from the gauging. It is a non-trivial fact that the theory associated with two different degenerations of the fourth punctured disc are related by Seiberg duality. The special assignment of the superpotential is crucial for this fact. Let us check this for  $l = 2$  (Fig. 24). In gauging two three punctured discs, there would be a new superpotential term for the newly formed cycle. Now let's first do Seiberg duality on node  $a$  and  $b$ , since they have  $N_f = 2N$ . After integrating out the massive fields, the gauge group  $c$  and  $d$  now has flavor  $N_f = 2N$  and we can do Seiberg

<sup>14</sup> This theory has nice application to 3d hyperbolic geometry and 3d  $\mathcal{N} = 2$  gauge theories [31].

duality on these nodes, and the final dual theory is exactly the same as the one defined by another degeneration limit of the fourth punctured disc. The general case can be found in [32, 33].

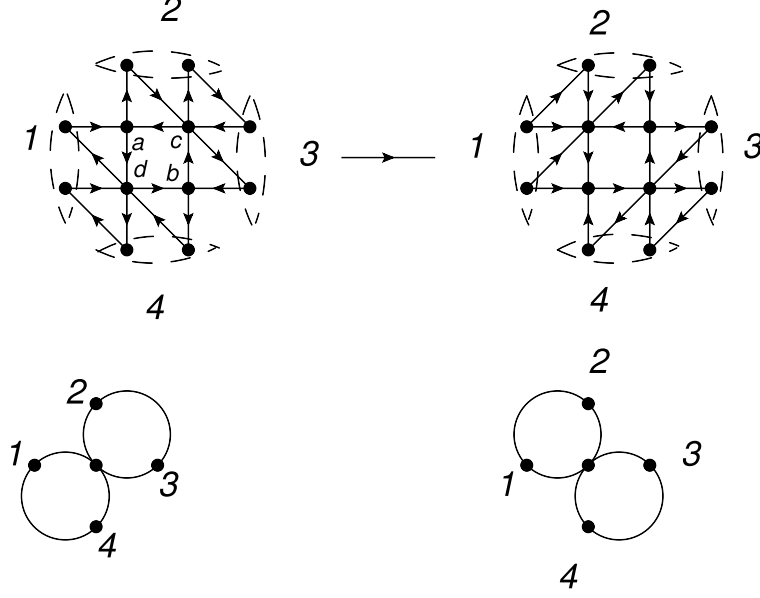


**Figure 23.** One first do Seiberg duality on node  $a$  and  $b$ , and then do Seiberg duality on node  $c$  and  $d$ , the dual quiver is the same as the one defined by another degeneration limit.

In the description above all the marked points are identical, however we can generalize this and use different punctures labeled by rank  $l$  Young tableaux. The corresponding three punctured disc theory and the Seiberg duality are described in [32, 33].

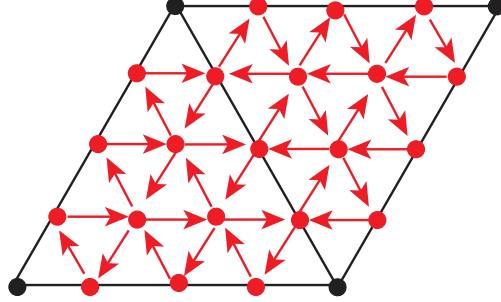


**Figure 24.** The theory  $\mathcal{T}_{\Delta}^{M=3}$  for a disc with four punctured is obtained by gluing two triangle theories  $\mathcal{T}_{\Delta}^{M=3}$ .

### 3.2 Ideal Triangulation

Now let us extend the definition of the theory to higher genus surface. This definition will be equivalent to the previous one if the genus is zero. Definition of our theory involves a triangulation of the surface, however we show that theories defined from different triangu-

lations are related by a sequence of local operations called a flip. The flip matches perfectly with the basic Seiberg duality, hence they define a unique IR fixed point

To define our theory we need to fix an ideal triangulation of  $\Sigma$ . An ideal triangulation is defined using arcs [34]. A simple arc  $\gamma$  in  $\Sigma$  is a curve such that

- a. the endpoints of  $\gamma$  are marked points;
- b.  $\gamma$  does not intersect itself, except at the endpoints;
- c.  $\gamma$  is disjoint from the marked points and the boundary.

We also require the arc  $\gamma$  is not contractible into the marked points or onto the boundary. Each arc is considered up to isotopy. Two arcs are called compatible if they do not intersect in the interior of  $\Sigma$ . A maximal collection of distinct pairwise arcs is called an *ideal triangulation*, see Fig. 25 for examples. An edge is called external if it is isotopic to a segment of the boundary, otherwise it is called internal.

It is not hard to get the following formula for the number of total edges

$$6g + 3b + \# |M_{\text{boundary}}| - 6 ,$$

where as defined previously  $g$  ( $b$ ) is the genus (the number of boundary components) of  $\Sigma$ , respectively. The number of internal edges is  $6g + 3b - 6$ , and there are a total of  $\# |M_{\text{boundary}}|$  external edges.

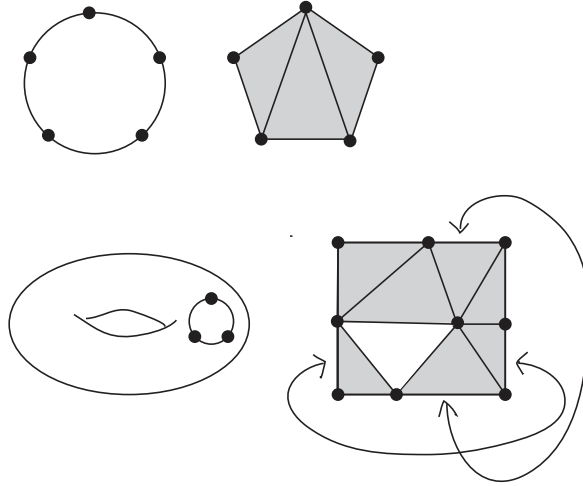


**Figure 25.** A bordered Riemann surface with marked points (a disc with five marked points and a torus with three marked points), its triangulation and the dual graph. The triangles are represented by gray regions, and there is no triangle in the white region.

### 3.2.1 The Definition of the Theories

Given a triangulation, we have the following rules for defining the 4d  $\mathcal{N} = 1$  SCFT:

1. Assign a  $SU(N)$  gauge group to each internal edge, and assign a  $SU(N)$  flavor group to each external edge.
2. There is a bifundamental chiral superfield between two gauge groups (or flavor groups) if the two corresponding edges are in the same triangle of the triangulation. The

orientation of the chiral is determined by the orientation of the triangle (we take clockwise orientation), i.e, if edge  $a$  is before edge  $b$  in the triangle, then the chiral is pointing quiver node  $b$ .

3. There is a cubic superpotential term for the three chirals in the same triangle.

Although the above definition looks quite different from previous subsection, they actually define the same theory. We have summarized the rules in Table 2.

**Table 2.** Summary of the rule

4d gauge theory	triangulation
$SU(N)$ symmetry	edge
gauge symmetry	internal edges
global symmetry	external edge
bifundamental and superpotential	triangle

### 3.2.2 Seiberg Duality is a Flip

The definition of  $\mathcal{T}_\Sigma$  to this point depends explicitly on the choice of the triangulation, and we in general have different Lagrangians when we choose different triangulations. However, different triangulations are related by local moves called flips (Fig. 26), and such a flip is indeed the basic Seiberg duality we considered in the last subsection. Therefore, the theories from different triangulations are related by a sequence of Seiberg duality, and our IR SCFT does not depend on the choice of the triangulation.

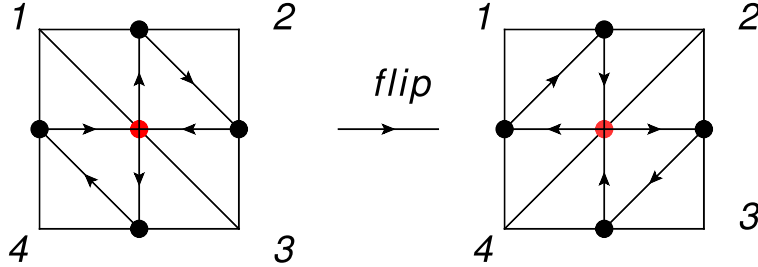


**Figure 26.** The Seiberg duality is interpreted as flip.

We can also generalize our definition by replacing the  $\mathcal{T}_\Delta$  by  $\mathcal{T}_\Delta^l$  theories, just as in section 3.1.

Finally, let us comment on the relation with the BPS quivers for the Gaiotto theories (see e.g. [34, 35]). When we dimensionally reduce our 4d  $\mathcal{N} = 1$  theory to 1d, we have a quantum mechanics, which is almost the same as the effective theory of the 1/2 BPS particles of 4d  $\mathcal{N} = 2$  SCFT. In the latter context a Seiberg duality of 4d  $\mathcal{N} = 1$  theory is interpreted as a quiver mutation which describes the wall crossing phenomena.

There is a major difference, however. The difference is that in 4d there is a non-trivial constraint from the existence of consistent IR superconformal R-charges. Indeed,

we now argue that if the Riemann surface has an empty boundary, there are gauge invariant operators with R-charge 0, and hence the 4d theory is problematic.<sup>15</sup>

To see this, it is enough to look at a three punctured disc with a bulk puncture. The triangulation and the field theory is shown in Fig. 27. If require the  $\beta$ -function to vanish and the superpotential to have R-charge 2 (more on this in section 4.1), it is easy to find that the gauge invariant operator  $\text{Tr}(XZY)$  has  $R$ -charge zero, which invalidates the 4d interpretation. However, this theory is perfectly fine as the BPS quiver.

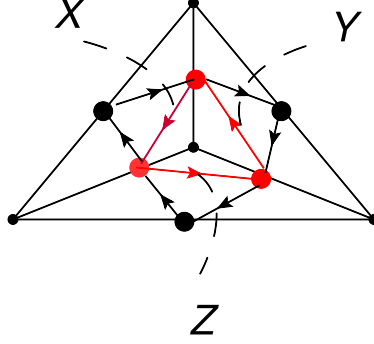


**Figure 27.** The gauge invariant operator  $\text{Tr}(XZY)$  has  $r$  charge 0 in the IR, and violates the unitarity bound.

### 3.3 Bipartite Graph

We now show that an ideal triangulation can be translated into a bipartite graph defined on the corresponding Riemann surface, thus making contact with the contents of section 2. The idea is very simple; we are going to define a network on each triangle and define how networks are glued together (Fig. 28).

Let us start with the quiver diagram of the triangle theory. We place a black (white) vertex at the small triangle with clockwise (counterclockwise) orientation. We also need to place white vertices on the boundary. The network is formed by connecting the black and white vertices if there is a quiver arrow between them. The gluing is achieved by identifying the white vertices. Such constructions are found in [32, 33]. We assign a superpotential term to any vertices of the network. We can also verify that a flip of the triangulation is equivalent to a square move.

We can compute the permutation for the bipartite graph, following the methods explained in section 2.4. For example, if we have a  $n$ -punctured disc, then the theory  $\mathcal{T}_{\Sigma}^{l=1}$  gives a permutation  $\pi : i \rightarrow i + 2$  modulo  $n$ . We also find that the integer  $k$  in (2.4) is given by  $k = 2$ , and hence this permutation corresponds to a cell of  $(\text{Gr}_{2,n})_{\geq 0}$ .

## 4 Properties of The Theories

In this section we make preliminary comments on the superconformal IR R-charges and the 4d superconformal indices of our theories. More detailed study of our theories will be

<sup>15</sup>We would like to thank S. Razamat for discussion on this issue.



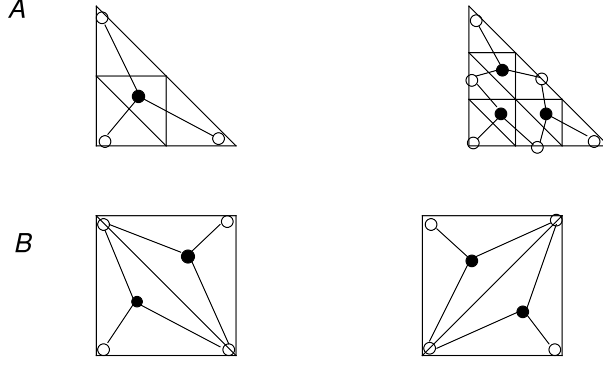


**Figure 28.** We assign a network to each triangle in the triangulation, and glue them together.

deferred for future work.

#### 4.1 R-charge

Let us next comment on the IR R-charges for the superconformal  $U(1)_R$ -symmetry. It should satisfy the following two constraints.

First, the  $\beta$ -function for Yukawa couplings vanish. This is the same as the requirement that the R-charge of the superpotential, and therefore any term in the superpotential, is normalized to be 2:

$$\sum_{e \in v} R_e = 2, \quad (4.1)$$

for any internal vertex of the quiver diagram.

Second, the  $\beta$ -functions for the gauge coupling vanish. From the NSVZ  $\beta$ -function, which in our case could be written as

$$\frac{d}{d \log \mu} \frac{1}{g_v^2} = \frac{N}{1 - g_v^2 N / 8\pi^2} \left[ 3 - \frac{1}{2} \sum_{e \in v} (1 - \gamma_e) \right], \quad (4.2)$$

where the anomalous dimension  $\gamma_e$  is related to the R-charge by  $\gamma_e = 3R_e - 2$ . From this condition, we have

$$\sum_{e \in V} (1 - R_e) = 2. \quad (4.3)$$

In general it is a non-trivial problem to see if there are physical solutions to these equations (recall the discussion in section 3.2.2).

Let us assume that the bicolored graph is reduced and planar. We can solve these constraints by assigning parameters to zig-zag paths. This is taken from the discussion of the torus case in [36, section 2.4], which originally goes back to [27].

Let us assign a  $2\pi$ -periodic angle  $\theta_i$  to each zig-zag path. We would like to determine the R-charge for a bifundamental field associated  $X_e$  with an edge  $e$  of the bipartite graph. Now note that for any edge there are exactly two zig-zag paths going through it. Then the

R-charge for  $X_e$  is simply defined to be the relative angles of the two zig-zag paths. The two conditions (4.1), (4.3) then follows from the facts that the total angle around a vertex is  $2\pi$ , and that the sum of exterior angles of a polygon is  $2\pi$ .

Note that this parametrization does not guarantee that the resulting R-charges are in the physical range. This happens, for example, when the graph is non-reduced; the R-charge of the bifundamental field is zero when there is a self-intersection of a zig-zag path.

## 4.2 Superconformal Index and Spin Chains

Let us also comment on the 4d superconformal index [37, 38] of our theories.

The superconformal index is a twisted partition function (Witten index) on  $S^1 \times S^3$ , and depends on several chemical potentials. For 4d  $\mathcal{N} = 1$  theories we have two chemical potentials  $t, y$  for combinations of spins and energy commuting with the supercharge, and a set of chemical potentials  $u_i$  for global symmetries.

Since the index is independent of continuous deformations of the Lagrangian, UV computation matches with the IR computation. This means this index is invariant under the moves of bicolored networks, and is determined purely from the IR fixed point. The invariance of the index under the Seiberg duality and Higgsing can also be verified explicitly, in exactly the same argument found in [36], under the parametrization of section 4.1.

In [36, 39] a relation between the 4d superconformal index and the partition function of a 2d integrable spin system has been proposed for the torus case. It is straightforward to adopt the argument there to the current setup, and we have a similar relation

$$\mathcal{I}_{4d} = Z_{2d \text{ spin}} . \quad (4.4)$$

The spin system on the right hand side of (4.4) is defined on a quiver diagram, which in our case is realized on the bordered Riemann surface. The spins reside at the vertices of the quiver diagram, and are  $U(1)^{N-1}$ -valued. These are precisely the integral variables of the matrix model representations of the index, or more physically the Polyakov loop along the thermal  $S^1$ .

The interactions for the spins are determined by the 1-loop determinants; the vector-multiplet determinants correspond to the self-interaction of the spins, and the hypermultiplet determinants, associated with an edge of the quiver diagram, represent the nearest-neighbor interaction among the spins.

The remarkable property of this spin chain is that they are integrable [40, 41]; the square move is translated into the double Yang-Baxter move of the zig-zag paths (or of strands), which follows from integrability, i.e. invariance of the partition function under the Yang-Baxter move. The relation (4.4) is reminiscent of the relation between 4d superconformal index for  $\mathcal{N} = 2$  Gaiotto theories and 2d TQFT [42, 43].

It would be interesting to work out the reduction of our 4d superconformal index to 3d  $S^3$  partition function [44–46] or 3d superconformal index [47]. We expect to find a connection with the geometry of some hyperbolic 3-manifold, probably along the lines of [36, 39].

## 5 Outlook

In this paper we defined a new class of 4d  $\mathcal{N} = 1$  SCFTs from reduced planar bicolored networks. We believe that this has opened up an exciting research direction. There are many open problems we could ask on our theories, some of which are listed here.

First and foremost, the question is whether or not our theories flow to a nontrivial IR fixed point. We have furthermore made several amazing statements from the combinatorial methods, e.g. some extremely complicated theories actually flow to the trivial theory. It would be interesting to study the IR properties of our theories by direct physical methods. For example, can we use the  $a$ -maximization to compute the IR R-charge? What are values of the central charges of  $a$  and  $c$ ? What does the vacuum moduli space look like? Are there any marginal deformations of the IR fixed point? What happens if we change the ranks of the gauge group to be unequal, and cause a cascade of Seiberg dualities? Do our theories have brane realizations, perhaps with gravity dual? Can we define similar theories in 3d with Chern-Simons terms?

In addition to the moves preserving the IR fixed point, we could consider operations on the bipartite graph which changes the fixed point. An example is to remove an internal edge. Physically, this turns on an expectation value of the fields represented by this edge. Now the theory flows to another fixed point, and it is remarkably simple to combinatorially identify the resulting IR fixed point using the moves and reductions.

For the case of higher genus Riemann surfaces, we have started with a Riemann surface and studied interesting networks and the corresponding gauge theories. However, the story will be much more fruitful if we start with a random network on Riemann surfaces, to identify the global data characterizing a network, and to determine if the two theories are the same in the IR. We believe our current understanding of the planar network is a key to the generalization. Since one may cut the Riemann surface into a disc with boundary points, and then gluing back the boundary points in the end, the understanding of the planar case should be really useful in extending the whole story.

In our characterization of the IR fixed point we have unexpectedly encountered a cell of the totally non-negative Grassmannian. However, in our story we have not made use of the actual geometrical data of the Grassmannian, for example the coordinate on them. To take this into account we need to incorporate weights to the edges of the bipartite graph. It is tempting to identify this weight with the R-charges with the edge variables.

The same network as in our paper plays an essential role in a number of physical contexts, including the scattering amplitude and the wall crossing phenomena. In each case the same mathematics, for example, cluster algebras [48, 49], play crucial roles. It is natural to ask whether there is any direct physical relations between them, i.e. whether there is a map between the calculable observables.

## Acknowledgments

We would like to thank Shlomo S. Razamat for initial collaboration and for numerous inputs. We also thank Nima Arkani-Hamed for stimulating discussion, and for sharing

some of the results of [25] prior to publication. This research is supported in part by Zurich Financial services membership and by the U.S. Department of Energy, grant DE-FG02-90ER40542 (DX), and by Princeton Center for Theoretical Science (MY).

## References

- [1] J. Drummond, J. Henn, G. Korchemsky, and E. Sokatchev, *Dual superconformal symmetry of scattering amplitudes in  $N=4$  super-Yang-Mills theory*, *Nucl.Phys.* **B828** (2010) 317–374, [[0807.1095](#)].
- [2] K. A. Intriligator and N. Seiberg, *Mirror symmetry in three-dimensional gauge theories*, *Phys.Lett.* **B387** (1996) 513–519, [[hep-th/9607207](#)].
- [3] A. Hanany and E. Witten, *Type IIB Superstrings, BPS Monopoles, and Three- Dimensional Gauge Dynamics*, *Nucl. Phys.* **B492** (1997) 152–190, [[hep-th/9611230](#)].
- [4] D. Gaiotto,  *$N=2$  dualities*, [0904.2715](#).
- [5] D. Gaiotto, G. W. Moore, and A. Neitzke, *Four-dimensional wall-crossing via three-dimensional field theory*, *Commun.Math.Phys.* **299** (2010) 163–224, [[0807.4723](#)].
- [6] D. Gaiotto, G. W. Moore, and A. Neitzke, *Wall-crossing, Hitchin Systems, and the WKB Approximation*, [0907.3987](#).
- [7] Y. Terashima and M. Yamazaki,  *$SL(2,R)$  Chern-Simons, Liouville, and Gauge Theory on Duality Walls*, *JHEP* **1108** (2011) 135, [[1103.5748](#)].
- [8] Y. Terashima and M. Yamazaki, *Semiclassical Analysis of the  $3d/3d$  Relation*, [1106.3066](#).
- [9] T. Dimofte and S. Gukov, *Chern-Simons Theory and  $S$ -duality*, [1106.4550](#).
- [10] T. Dimofte, D. Gaiotto, and S. Gukov, *Gauge Theories Labelled by Three-Manifolds*, [1108.4389](#).
- [11] S. Cecotti, C. Cordova, and C. Vafa, *Braids, Walls, and Mirrors*, [1110.2115](#).
- [12] T. Dimofte, D. Gaiotto, and S. Gukov, *3-Manifolds and  $3d$  Indices*, [1112.5179](#).
- [13] A. Hanany and K. D. Kennaway, *Dimer models and toric diagrams*, [hep-th/0503149](#).
- [14] S. Franco, A. Hanany, K. D. Kennaway, D. Vegh, and B. Wecht, *Brane dimers and quiver gauge theories*, *JHEP* **0601** (2006) 096, [[hep-th/0504110](#)].
- [15] S. Franco, A. Hanany, D. Martelli, J. Sparks, D. Vegh, *et al.*, *Gauge theories from toric geometry and brane tilings*, *JHEP* **0601** (2006) 128, [[hep-th/0505211](#)].
- [16] C. E. Beasley and M. R. Plesser, *Toric duality is Seiberg duality*, *JHEP* **0112** (2001) 001, [[hep-th/0109053](#)].
- [17] Y. Imamura, H. Isono, K. Kimura, and M. Yamazaki, *Exactly marginal deformations of quiver gauge theories as seen from brane tilings*, *Prog. Theor. Phys.* **117** (2007) 923–955, [[hep-th/0702049](#)].
- [18] M. Yamazaki, *Brane Tilings and Their Applications*, *Fortsch.Phys.* **56** (2008) 555–686, [[0803.4474](#)]. Master’s Thesis.
- [19] B. Feng, Y.-H. He, K. D. Kennaway, and C. Vafa, *Dimer models from mirror symmetry and quivering amoebae*, *Adv.Theor.Math.Phys.* **12** (2008) 3, [[hep-th/0511287](#)].
- [20] A. Postnikov, *Total positivity, Grassmannians, and networks*, [arXiv:math/0609764](#).

- [21] N. Seiberg, *Electric - magnetic duality in supersymmetric nonAbelian gauge theories*, *Nucl.Phys.* **B435** (1995) 129–146, [[hep-th/9411149](#)].
- [22] S. Franco, *Bipartite Field Theories: from D-Brane Probes to Scattering Amplitudes*, [1207.0807](#).
- [23] D. Berenstein and M. R. Douglas, *Seiberg duality for quiver gauge theories*, [hep-th/0207027](#).
- [24] D. Thurston, *From dominoes to hexagons*, [math/0405482](#).
- [25] N. Arkani-Hamed, J. L. Bourjaily, F. Cachazo, A. Goncharov, A. Postnikov, and J. Trnka, *Positive Grassmannian and Scattering Amplitude*, to appear.
- [26] K. D. Kennaway, *Brane Tilings*, *Int.J.Mod.Phys.* **A22** (2007) 2977–3038, [[0706.1660](#)].
- [27] A. Hanany and D. Vegh, *Quivers, tilings, branes and rhombi*, *JHEP* **0710** (2007) 029, [[hep-th/0511063](#)].
- [28] A. Goncharov and R. Kenyon, *Dimers and cluster integrable systems*, [1107.5588](#).
- [29] A. Hanany and R.-K. Seong, *Brane Tilings and Specular Duality*, [1206.2386](#).
- [30] V. Fock and A. Goncharov, *Moduli spaces of local systems and higher Teichmüller theory*, *Publ. Math. Inst. Hautes Études Sci.* (2006), no. 103 1–211.
- [31] T. Dimofte, M. Gabella, D. Xie, and M. Yamazaki, in progress.
- [32] D. Xie, *Network, Cluster coordinates and  $N=2$  theory I*, [1203.4573](#).
- [33] A. Goncharov, *Ideal webs and moduli spaces of local systems on surfaces*, to appear.
- [34] S. Fomin, M. Shapiro, and D. Thurston, *Cluster algebras and triangulated surfaces. I. Cluster complexes*, *Acta Math.* **201** (2008), no. 1 83–146.
- [35] S. Cecotti and C. Vafa, *Classification of complete  $N=2$  supersymmetric theories in 4 dimensions*, [1103.5832](#).
- [36] M. Yamazaki, *Quivers, YBE and 3-manifolds*, *JHEP* **1205** (2012) 147, [[1203.5784](#)].
- [37] C. Romelsberger, *Counting chiral primaries in  $N = 1$ ,  $d=4$  superconformal field theories*, *Nucl.Phys.* **B747** (2006) 329–353, [[hep-th/0510060](#)].
- [38] J. Kinney, J. M. Maldacena, S. Minwalla, and S. Raju, *An Index for 4 Dimensional Super Conformal Theories*, *Commun. Math. Phys.* **275** (2007) 209–254, [[hep-th/0510251](#)].
- [39] Y. Terashima and M. Yamazaki, *Emergent 3-manifold from 4d Superconformal Index*, [1203.5792](#).
- [40] V. V. Bazhanov and S. M. Sergeev, *A Master solution of the quantum Yang-Baxter equation and classical discrete integrable equations*, [1006.0651](#).
- [41] V. V. Bazhanov and S. M. Sergeev, *Elliptic gamma-function and multi-spin solutions of the Yang-Baxter equation*, *Nucl.Phys.* **B856** (2012) 475–496, [[1106.5874](#)].
- [42] A. Gadde, E. Pomoni, L. Rastelli, and S. S. Razamat, *S-duality and 2d Topological QFT*, *JHEP* **1003** (2010) 032, [[0910.2225](#)].
- [43] A. Gadde, L. Rastelli, S. S. Razamat, and W. Yan, *The 4d Superconformal Index from  $q$ -deformed 2d Yang-Mills*, [1104.3850](#).
- [44] F. A. H. Dolan, V. P. Spiridonov, and G. S. Vartanov, *From 4D Superconformal Indices to 3D Partition Functions*, *Phys. Lett.* **B704** (2011) 234, [[1104.1787](#)].

- [45] A. Gadde and W. Yan, *Reducing the 4d Index to the  $S^3$  Partition Function*, [1104.2592](#).
- [46] Y. Imamura, *Relation between the 4d superconformal index and the  $S^3$  partition function*, *JHEP* **1109** (2011) 133, [[1104.4482](#)].
- [47] F. Benini, T. Nishioka, and M. Yamazaki, *4d Index to 3d Index and 2d TQFT*, [1109.0283](#).
- [48] S. Fomin and A. Zelevinsky, *Cluster algebras. I. Foundations*, *J. Amer. Math. Soc.* **15** (2002), no. 2 497–529 (electronic).
- [49] H. Derksen, J. Weyman, and A. Zelevinsky, *Quivers with potentials and their representations. I. Mutations*, *Selecta Math. (N.S.)* **14** (2008), no. 1 59–119.